IX International Conference on Particle-Based Methods
PARTICLES 2025
J. Bonet, M. Cremonesi, A. Franci, A. Gil (Eds)

# INVESTIGATIONS REGARDING THE INFLUENCE OF PARTICLE SHAPE ON THE NUMERICAL SIMULATION OF AIR PLUVIATION USING THE DEM METHOD

**NATASCHA HEIM[*] AND SASCHA HENKE[†]**

[*] Helmut-Schmidt-University
Faculty for mechanical and civil engineering, professorship for geotechnics
Postfach 70 08 22, 22008 Hamburg, Germany
e-mail: heimn@hsu-hh.de, web page: https://www.hsu-hh.de/geot/

[†] Helmut-Schmidt-University
Faculty for mechanical and civil engineering, professorship for geotechnics
Postfach 70 08 22, 22008 Hamburg, Germany
e-mail: sascha.henke@hsu-hh.de, web page: https://www.hsu-hh.de/geot/

**Key words:** Granular Material, Sand, DEM, Sand pluviation, Particle shapes.

**Abstract.** Air pluviation or sand raining is a method in geotechnics to create homogenous sand samples [1]. To investigate the behavior of the sand particles during pluviation, DEM (discrete element method) can be used due to its ability to realistically model particle interactions [2] with other sand particles or the pluviation equipment. These interactions are in turn influenced by the material as well as interaction properties and particle scaling. However, particle shape also influences the behavior such that realistically considering real-world particles' shapes may improve modelling of the pluviation process.

To investigate the influence of particle shape on the simulation of air pluviation, three different numerical representations for sand particles will be used: (I) homogenous sand with spherical particles, (II) homogenous sand with uniform non-spherical particle shape, representing the average particle shape, and (III) heterogenous sand with varying particle shapes. The non-spherical particles are created using bonded spheres. For investigation of the pluviation process four partial processes were identified which are most likely to be influenced by particle shape: (I) the outflow out of the sieve, which regulates deposition intensity, (II) interactions with the diffusor sieves, which distribute the sand homogeneously over the sample surface, (III) free falling and the resulting particle interactions as well as (IV) the resulting sample density. For these processes, the impact of particle shape will be determined, including resulting particle velocities, angular velocities as well as the reached sample density. The results will, were applicable, be compared to results of physical experiments for further evaluation and validation.

## 1 INTRODUCTION

Air pluviation is a method in geotechnics used for creation of homogenous sand samples. During execution, a sand rain is created over a sample surface. The impact of the sand grains

compacts the lower layers and thus influence sample density. This process is mainly dependent on the interactions of particles with each other as well as with the pluviation set-up. During these interactions, particle collisions influence the movement of the particles in the system. Particle movements include translational movements, but also rotational. As particle shape influences the collisions, it also influences particle movements and therefore the pluviation process. Furthermore, the particle shape also influences the particle packing and the resulting sample density.

Investigating the pluviation process numerically, it is generally best to choose a method capable of directly depicting collisions. Therefore, a particle-based method, like discrete element method (DEM) is suitable. However, particle shape is generally not realistically depicted during DEM simulations. Usually, particles are depicted as spheres, and properties resulting from particle shape and surface structure are simplified by means of friction coefficients, such as increased sliding and rolling friction. However, this only partially resembles realistic particle behavior. On the other hand, it is also possible during DEM simulations to consider different particle shapes, which would result in better description of particle movements. But as shaped particles are generally created as an agglomerate of several smaller particles, their use significantly increases simulation time as well as the required computational resources.

Therefore, the present investigations are aimed at identifying differences between spherical and non-spherical particles during the simulation of sand pluviation. For this, comparable simulations are conducted for three different particle shapes: spherical or round particles, uniform non-round particles, where all particles share the same, non-spherical shape, and non-uniform non-round particles, where different particle shapes are considered.

## 2 SAMPLE SAND

### 2.1 Physical sand

The sand used for these investigations was a natural sand mainly consisting of quartz. The grains were sieved to values between 0.5 mm and 1 mm, which allowed for easier simulations, because finer particles did not need to be modelled. To determine particle shape, dynamic image analysis was used. For this, a small sample of the sand was analyzed using the CamSizer X2 from Mictrotrac [3], determining a 2D-shadow of the particles showing particle sizes as well as shapes, which then were used as a basis for the numerical simulations.

### 2.2 Round numerical sand

For these investigations, it is important to be able to depict the shape of the particles. For this, the three different representations round, non-round with a uniform shape and non-round particles with different shapes were used. If the particles were modelled considering their actual size, the computational requirements would be too large. Therefore, the particles were scaled with a scaling factor of five.

First, spherical particles were modelled. This is the most common depiction of particles in DEM simulations of sand, due to the increased simplicity and therefore reduced required computational time. However, simply depicting one uniform particle size does not show the behavior of the particles during pluviation, especially the achieved sample density [4].

Therefore, scaling of the physical sample needs to be replicated as well as possible, which was realized by using three different particles sizes. To determine both the particle sizes as well as the particle portion required, a weight-equal distribution of the sand particles between 0.5 mm and 1.0 mm was assumed. This distribution was divided into three parts leading to particle sizes of 0.583 mm, 0.75 mm and 0.917 mm, defining scaling of five to 2.92 mm, 3.75 mm and 4.58 mm. Determining the portion of the particles, the following equations were used, where χ is the portion and d the diameter of the particles. This leads to parts of 57.8 % of 2.92 mm particles, 27.2 % of 3.75 mm particles and 15.0 % of 4.58 mm particles.

$$d_1^3 * \chi_1 = d_2^3 * \chi_2 = d_3^3 * \chi_3 \tag{1}$$

$$\chi_1 + \chi_2 + \chi_3 = 1$$

## 2.3 Uniform non-round numerical sand

The non-round sand particles were created using spherical particles and bonds. To recreate the shapes of the physical sand particles, an average ratio of particle width to particle length was determined to 0.715. However, in geotechnics, grain size is generally determined by particle width. If this would have been simply applied to the numerical particles all shaped particles would be significantly larger than the spherical ones. This would lead to further simulation differences. To account for this, scaling of the particle was applied as such, as that the average length and width of the particles was equal to the diameter of the round particles. The particle ratios were also taken from the round particles. With this, a medium particle with a length of 4.37 mm and a width of 3.13 mm was created. The small and large particles were achieved by scaling them in the simulation, with a scaling factor of 0.7787 for the small particles and 1.2213 for the large particles. The same portions as for the spherical particle were used.

When creating the actual particles, first a spheroid with one axis being the particle length and two axes being the particle width was created, which should best depict the particle shape determined using the CamSizer. This shape was then randomly filled with non-overlapping particles with a diameter of 1 mm. These particles were then connected via bonds, also having a diameter of 1 mm. The bonds are created between all particles, with distances of up to 1 mm. The sequence for particle creation is shown figure 1.

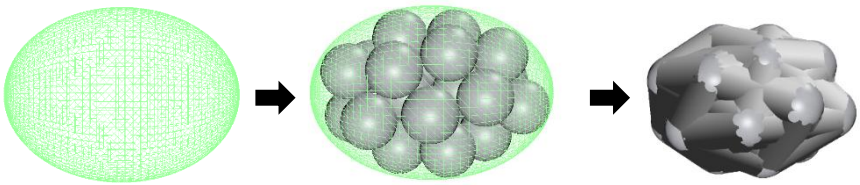

**Figure 1: Steps for creating non-round particles through bonds**

## 2.4 Non-uniform, non-round numerical sand

When creating non-uniform, non-round particles, not only variation of particle sizes but also of particle shapes of the physical sand needs to be considered. For this, the particle shapes were merged into different subgroups with width to length ratios of 1 to 0.7, 0.7 to 0.5 and 0.5 to 0,

which correspond to the width to lengths ratios of 0.8, 0.6 and 0.4, which represent the particle shape. For each subgroup the percentage of particles in the physical sand were determined. The resulting particles can be seen in table 1. Afterwards, the scaling factors and portions of the other particles were applied.

**Table 1**: Particle geometries of uniform non-round sand particles

| Particle Shape | Particle length | Particle width | Percentage |
|---|---|---|---|
| 0.8 | 4.17 mm | 3.33 mm | 31.9 % |
| 0.6 | 4.69 mm | 2.81 mm | 49,0 % |
| 0.4 | 5.36 mm | 2.14 mm | 19.1 % |

## 3 PHYSICAL EXPERIMENTS

### 3.1 Physical Pluviation test stand

To be able to compare the simulation results and to evaluate them regarding the applicability to real-life, a comparison experiment was used. This physical experiment was conducted using an existing pluviation test stand, shown in figure 2. In the test stand, the sand is first filled into a silo, which holds the material before pluviation. Underneath the silo, a slide dampener is attached, which opens at the beginning of the experiment. Below the slide dampener, a chamber with two calming trays is attached. The function of the calming trays, which consist of metal plates with round openings, is to mix the sample before reaching the sieve, to avoid inhomogeneities possibly being created while filling the silo. Underneath the calming trays, the sieve is attached. The sieve is responsible for adjusting the deposition intensity, which is the mass of sand falling on the sample for a specific area and time. The deposition intensity is the primary factor influencing bulk density of the created sample. Choice of the right sieve for the indented application therefore is of main importance. Following the sieve, a casing is created reaching to the sample container. In this casing, two diffusor sieves are attached underneath the sieve. The diffusor sieves consist of a quadratic mesh and are supposed to distribute the sand homogeneously over the sample surface. Finally, the sand falls into the sample container on the bottom of the pluviation test stand.

### 3.2 Pluviation settings and results

For pluviation experiments in this study, a sieve with 5 mm openings covering 10 % of the surface was chosen. The two diffusor sieves were created using a 6 mm mesh and were attached 50 and 100 mm underneath the sieve, with the second diffusor rotated by 45°. The sieve and the diffusor sieves were consistently held 200 mm above the sample container, leading to falling heights between 300 and 100 mm from the lowest diffusor sieve during pluviation. This set-up resulted in a deposition intensity of 12.2 $kg/m^2 \cdot s$ and a samples bulk density of 1690 $kg/m^3$. Direct particle movements could, however, not be observed.

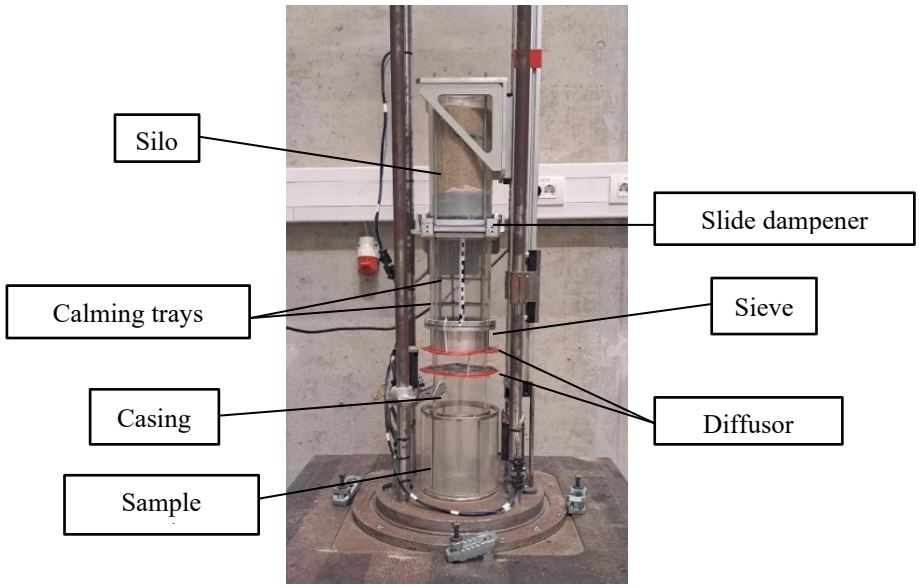


**Figure 2**: Physical pluviation test stand

## 4 SET-UP OF THE NUMERICAL SIMULATIONS

### 4.1 General simulation aspects

All simulations were conducted using MUSEN [5] an open-source DEM program. Hertz-Mindlin was chosen as the contact model, which combines normal interactions of the Hertz theory and tangential interactions of Mindlin and Deresiewicz [6]. This is a common contact model used in DEM simulations [7]. The Hertz-Mindlin model considers six parameters: the three material parameters density, Young's modulus, and Poisson's ratio, and the three contact parameters coefficient of restitution, sliding friction and rolling friction. Contact parameters must be defined between all materials in the simulation. For the bonds, an elastic bond model was chosen. This allows to best depict grain behavior; plastic bonds would change the particle shapes over the simulation time, while elastic bonds with the same Young's modulus and Poisson's ratio as the particles allow to mimic the behavior of a non-round particle. Time step of the simulation is calculated as a tenth of the smaller time step, either Rayleigh time [8] or the critical time step for bonds after O'Sullivan and Bray [9].

### 4.2 Simulation parameters

In the simulations, only one other material than sand was be used, which is "steel". For this material, the material and contact parameters are based on literature values and were be varied for the simulations. Further, the parameters describing contact between steel and sands were also kept constant. The used values are summarized in table 2.

However, the material and contact parameters for the different sands need to be adjusted to the material used in the physical experiment. In previous investigations, the material properties of spherical particles were calibrated. Because here the influence of the particle shape is most likely negligible, they are also used for the non-round particles. For the contact parameters, the coefficient of restitution also was taken from these previous calibrations. The friction

coefficients, however, need to be adjusted. This is because particle shape significantly influences sliding and rolling friction. The used methods and results are discussed in section 4.3. Finally, the parameters determining breakage criteria of the bonds, namely normal and tangential strength, were both set to very high values. This was chosen not to depict real particle behavior, but to ensure that the particles do not break during pluviation as grain breakage is not expected during physical sand pluviation. The sand parameters (without friction) used in the numerical simulations are summarized in table 3.

**Table 2**: Material and contact parameters of steel

| Parameter | Unit | Value |
|---|---|---|
| Material parameters of steel | | |
| Density | kg/m³ | 7800 |
| Young's modulus | Pa | $2.1 * 10^{11}$ |
| Poisson's ratio | - | 0.285 |
| Contact parameters of steel on steel | | |
| Coefficient of restitution | - | 0.8 |
| Sliding friction | - | 0.2 |
| Rolling friction | - | 0.05 |
| Contact parameters of steel on sand | | |
| Coefficient of restitution | - | 0.8 |
| Sliding friction | - | 0.35 |
| Rolling friction | - | 0.08 |

**Table 3**: Non varied material and contact parameters of sands

| Parameter | Unit | Value |
|---|---|---|
| Density | kg/m³ | 2650 |
| Young's modulus | Pa | $4.0 * 10^{8}$ |
| Poisson's ratio | - | 0.30 |
| Normal strength | Pa | $10^{12}$ |
| Tangential strength | Pa | $10^{12}$ |
| Coefficient of restitution | - | 0.75 |

### 4.3 Parameter calibration

Calibrating the sliding and rolling friction, the angle of repose test was used. In the physical experiment, the sample sand was filled into a funnel, which is then slowly lifted. The resulting sand cone had a slope angle of 31.8° and straight slopes with a slightly rounded tip.

For the numerical simulation, the funnel was replaced with a hollow tube, in which a sample of the sand was created and then allowed to settle. Afterwards, the tube was slowly lifted such that the cone formed. Both, the shape and the angle of the cone were used during the calibration. The round particles were calibrated after eight simulations with an angle of 31.2°, the uniform non-round particles after 2 simulations with 32.3°, and the non-uniform, non-round particles after 6 simulations with 32.6°. The resulting sand cones can be seen in figure 3, while the resulting friction parameters are found in table 4. As expected, the sliding parameters of the shaped particles are lower than for round particles.

**Table 4**: Adjusted sliding and rolling friction parameters

| Particle shape | Sliding friction [-] | Rolling friction [-] |
|---|---|---|
| Round | 0.26 | 0.17 |
| Uniform, non-round | 0.15 | 0.08 |
| Non-uniform, non-round | 0.15 | 0.08 |

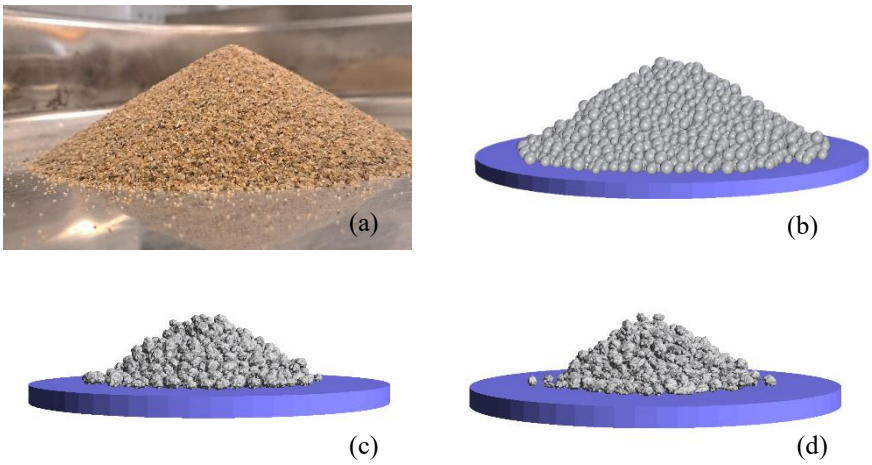


**Figure 3**: Angle of repose: (a) physical sand, (b) round particle, (c) uniform, non-round particles, (d) non-uniform, non-round particles

## 5 NUMERICAL SIMULATION OF SAND PLUVIATION

After parameter calibration, the pluviation simulations could be conducted. For this, some aspects of the pluviation set-up had to be adjusted. First, the calming trays are not modelled in the simulation, because the sample is randomly created, which avoids layering in the silo. Therefore, the slide dampener can directly be attached underneath the silo. Further, all simulation components need to be scaled up. For this, the same factor of five as for the particles is applied. However, to reduce the required computational time, the sample needs to be reduced in both diameter and height. While the height can simply be halved, resulting in falling heights between 250 mm and 150 mm, the diameter needs to be scaled more carefully, because the ratio of sieve opening and sample needs to be replicated. The chosen sieve in the physical experiment has an open area of 10 % with hole diameters of 5 mm. To replicate this in the simulation, the sieve opening needs to be scaled to 25 mm. When using only one opening, this means that the required sample diameter comes to 79 mm.

To analyze different parts of the simulation model, several analysis volumes were defined, which are shown in figure 4. These consist of the silo, zones before the first, after the first and after the second diffusor sieve, the free-falling and the sample. In each zone, particles experience different interactions etc. The zones help to better analyze the particles and agglomerates, which will be described in the following sections.

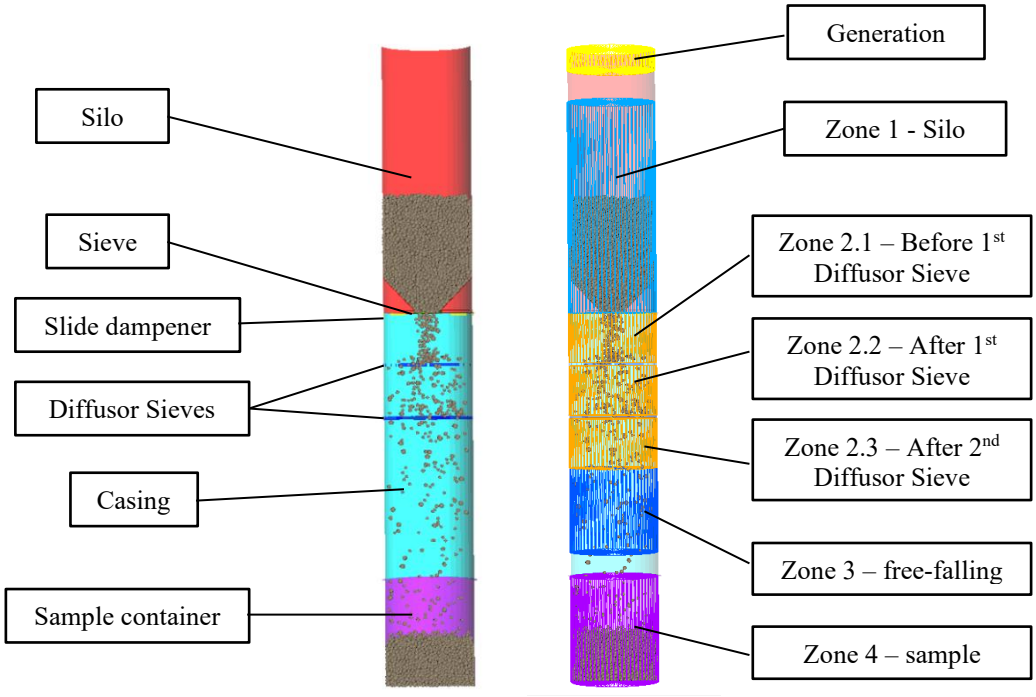


**Figure 4**: Left: structure of pluviation simulation, right: analysis volumes

## 5.1 Interaction with the sieve

When investigating the interactions with the sieve, two main aspects to be considered are the achieved deposition intensity and the behavior of the particles in and around the sieve opening.

The deposition intensity is determined by calculating the mass remaining in the silo at small time intervals in connection to the sample surface. Here, 23.2 kg/(m²·s) for the round particles, 34.6 kg/(m²·s) for the uniform, non-round particles and 33.1 kg/(m²·s) for the non-uniform, non-round particles were reached. These values are larger than the deposition intensity found during the physical experiment. This could be due particle scaling. In physical experiments, both absolute particle sizes as well as the largest particle sizes effect deposition intensity, which could also be a factor in the numerical simulations. This would also explain why the two non-round particle shapes show similar deposition intensities, as the same scaling methods were applied.

Another aspect that could affect deposition intensity is the particle direction when passing the sieve. Here, both the uniform and non-uniform particles are more likely to pass with their smaller surface turned towards the sieve. This is due to the sieve providing a narrow point in particle flow. This would also at least in part explain the increased deposition intensity of the particles: non-round particles have an effective lower diameter than the round particles when exiting the sieve. This behavior can also be seen in the rotational velocities above and below the sieve. For round particles, the rotational velocities are larger below the sieve, while for non-round particles they are higher above the sieve, where the particles shift into an optimal position. When passing the sieve, however, the non-round particles have lower rotational velocities. This can be seen in the figure 5, which shows the sieve area for all particle shapes

1 s after complete opening of the slide dampener. However, round particles show higher rotational velocities than the non-round particles both above and below the sieve. This is most likely due to the lack of particle shapes hindering particle rotation.

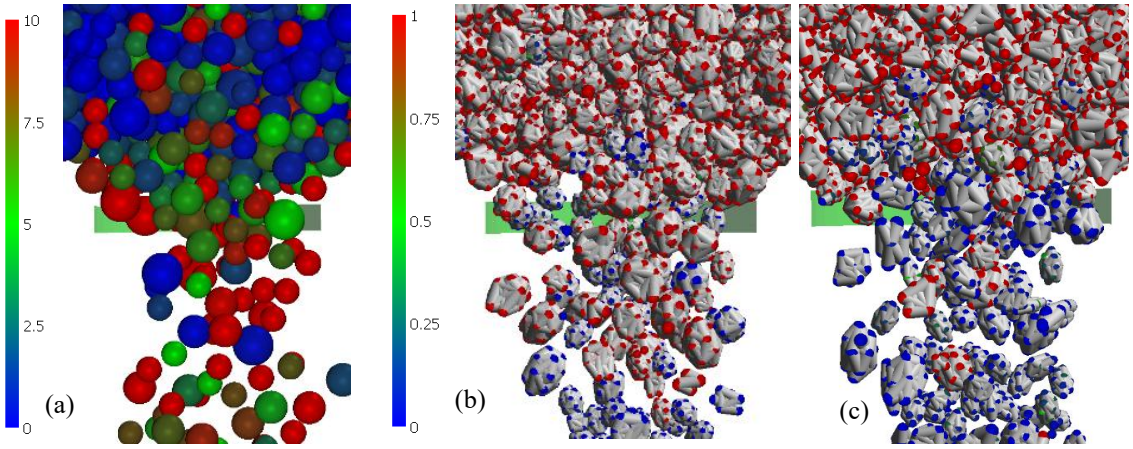


**Figure 5**: Rotational velocities during sieve passing (simulation time 3.2 s) (rad/s) (a) round, (b) uniform, (c) non-uniform

Contrary to this, the translational velocities of all particle shapes are very similar. In the area between sieve and first diffusor sieve, translational velocities were all around 0.6 m/s. Before the sieve, all velocities are very low during most of the pluviation process. Only during the final emptying of the silo, the velocities similarly increase for all particle shapes.

### 5.2 Interaction with diffusor sieves

When evaluating the interactions of different particle shapes, the effectiveness of the diffusor sieves needs to also be evaluated. Without a homogenous distribution, the sample does not form properly. Here, the diffusor sieves were effective for all particle shapes, meaning that the particle shape does not seem to effect the effectivity of the diffusor sieves.

When analyzing the translational velocities, all particles again show similar behavior and values. All translational velocities increase from 0.6 m/s to 0.95 m/s underneath the second diffusor sieve and are relatively consistent. The average translational velocity however varies regarding different particle shapes and over the simulation time. While the velocities are approximately equal for the non-uniform particles before the first and after the second diffusor sieve, they increase for the uniform and even further for the round particles. This is most likely due to the different behaviors during particle-particle and particle-geometry collision. The non-round particles are forced into a flow path due to their shape and interactions, which limits rotation. This is not the fact for round particles. Finally, variation of the rotational velocities is similar for all particle shapes, both over individual particles as well as simulation time. This is due to the random interaction of the particles. The rotational velocities before and after the diffusor sieves between simulation time 3.2 s and 4.2 s can be seen in figure 6.

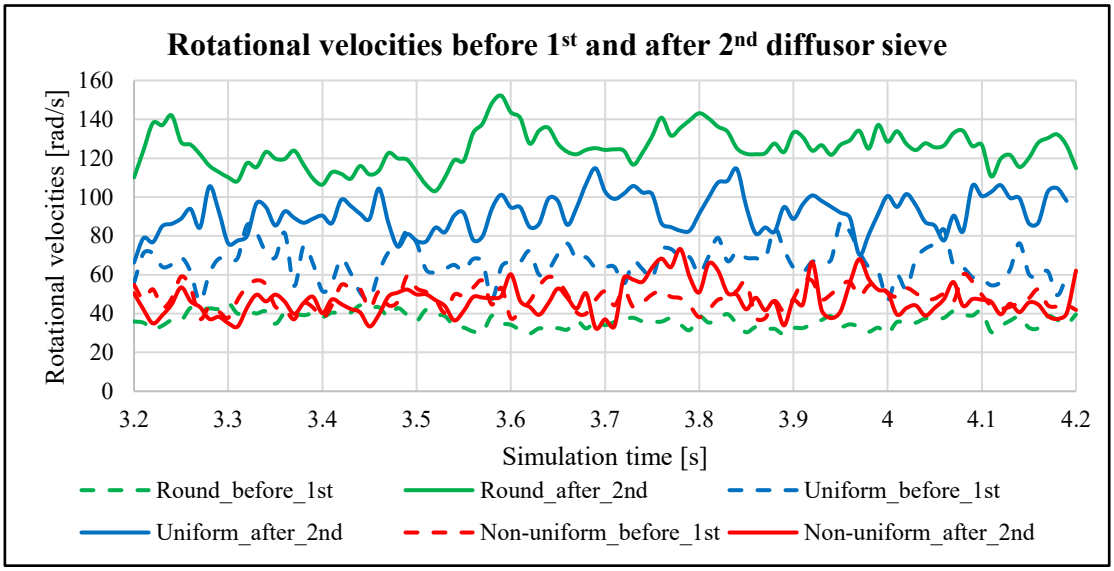


**Figure 6**: Rotation velocities before 1st and after 2nd diffusor sieve

### 5.3 Behavior during free-falling

During free-falling development of velocities has to be observed. Here, both translational and rotational velocities of small, medium and large particles were considered.

The behaviour of the translational velocities is consistent with the one described during interaction with the diffusor sieves. All particles, regardless of shape or size, show a similar average velocity of approximately 1.5 m/s. However, round particles show a slightly larger variation in falling velocities over time compared to non-round particles, though this variation is not very large with values varying under 10%. Translational velocities during free-falling for simulation time 3.2 s are shown in figure 7.

Regarding rotational velocities, round particles again show higher values. However, while the round particle averages showed no difference between different particle sizes, for the non-round particles rotational velocities were higher for larger particles. Further, rotational velocities were also slightly higher for uniform particles compared to the non-uniform ones. Finally, all particle shapes showed significant variations of rotational velocities over simulation time and between different particles.

### 5.4 Achieved sample density

Regarding sample density, for round particles, a density of 1490 kg/m³ was achieved. This is lower than the density seen in the physical experiment. Contrary to this, the density of the uniform sample was 2250 kg/m³ and for the non-uniform 1900 kg/m³. The large differences could be due to different influences. The main differences between simulation and experiment, are the upscaled particles and the lack of air resistance. Both could contribute to increased density for non-round sands. Another facet are higher rotational velocities of uniform particles.

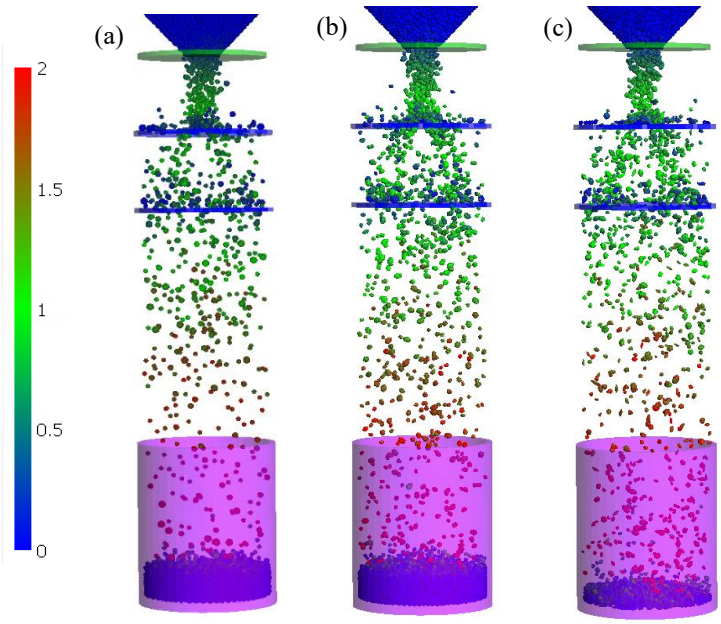


**Figure 7**: Translational velocities during free-falling [m/s] (simulation time 3.2 s), (a) round, (b) uniform, (c) non-uniform

Looking closer at the samples, another aspect might be the bedding of the particles, shown in figure 8. While uniform particles are packed very closely, non-uniform particles show a higher porosity, leading to lower densities. For round particles the density is even lower, because particle rotation is not a factor influencing packing. It is however an influence on the non-round sands, which is most apparent in the non-uniform sample. While particles with smaller width to length ratio are more likely to "lie flat" in the sample, rounder particles do not necessarily show this behavior.

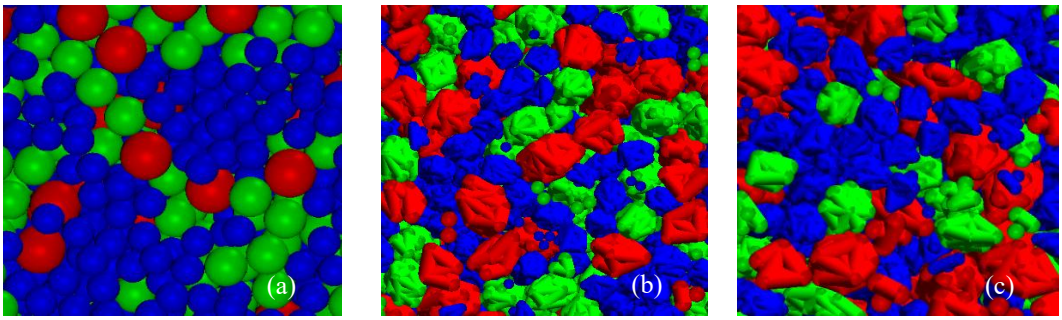


**Figure 8**: Particle bedding in the sample (red: large particles, green: medium particles, blue: small particles), (a) round, (b) uniform, (c) non-uniform

Finally, an interesting aspect is clustering of same size particles. This is especially apparent with round particles, showing a lot of clustering, especially with small particles. This effect reduces with non-round particles.

## 6 CONCLUSIONS

Simulation of sand pluviation with different particle shapes does lead to different results. While translational velocities do not seem to depend on particle shape, round particles do overestimate rotational velocities compared to non-round ones which better represent physical sands. Other aspects, such as the achieved deposition intensity, interactions during free-falling and with diffusor sieves also show differences. Here, the uniform non-round particles only show slight improvement compared to round particles. This is especially clear regarding the achieved sample, severely overestimating packing density. While this effect could be due to the specific particle shape, it is neither the less significant. Considering this, and the only very slight increase in computational time using non-uniform particles, the use of uniform non-round particles for DEM simulation of sand pluviation is not recommended. The use of non-round and non-uniform particles, best representing the variation of particle shape within a sample can, however, give more insight into different aspects of the pluviation process.

However, further investigations into the effect of particle shape on the simulation of pluviation is necessary. Here, mainly deposition intensity and sample packing needs to be investigated and further compared to physical experiments.

## REFERENCES


[1] Rad, N. and Tumay, M. 1987. Factors affecting sand specimen preparation by raining. *Geotechnical Testing Journal*, pp. 31-37. https://doi.org/10.1520/GTJ10136J

[2] Balamonica, K. and Goh, S. H. 2019. Characterisation of contact parameters of sand grains to be used for discrete element modelling. *E3S Web of Conferences 92*, 14002 (2019) IS-Glasgow 2019. https://doi.org/10.1051/e3sconf/20199214002

[3] Microtrac Tesch GmbH. 2025. *Particle Size and Shape Analyzer CamSizer X2*, last accessed on 08.08.2025 under https://www.microtrac.com/products/particle-size-shape-analysis/dynamic-image-analysis/camsizer-x2/

[4] Heim, N. and Henke, S. 2024. Effect of particle-size-scaling on particle interactions in DEM-simulations of sand in the context of air pluviation, in: *WCCM2024*. URL https://www.scipedia.com/public/Heim_Henke_2024a

[5] Dosta, M. and Skorych, V. 2020. msolids MUSEN v1.73.0 (2022) [Computer Program]. Available at https://msolids.net/musen/download/ (Downloaded 05.07.2023)

[6] Di Renzo, A. and Di Maio, F.P. 2004. Comparison of contact-force models for the simulation of collisions in DEM-based granular flow codes. *Chemical Engineering Science 59* (2004) 525–541. https://doi.org/10.1016/j.ces.2003.09.037

[7] Qin, R., Fang, H., Liu, F., Xing, D., Yang, J., Lv, N., Junlong, C. and Li, J. 2019. Study on Physical and Contact Parameters of Limestone by DEM. *IOP Conference Series: Earth and Environmental Science*. 252: 052110. DOI: http://dx.doi.org/10.1088/1755-1315/252/5/052110

[8] Burns, S. J., Piiroinen, P.T. and Hanley, K.J. 2019. Critical time step for DEM simulations of dynamic systems using a Hertzian contact model. *Int J Numer Methods Eng*. 2019; 119: 432–451. DOI: https://doi.org/10.1002/nme.6056

[9] O'Sullivan, C. and Bray, J.D. 2003. Selecting a suitable time step for discrete element simulations that use the central difference time integration scheme, *Engineering Computations 21*, 278-303. http://dx.doi.org/10.1108/02644400410519794